Conformations of Alanine-Based Peptides in Water Probed by FTIR, Raman, Vibrational Circular Dichroism, Electronic Circular Dichroism, and NMR Spectroscopy†

Reinhard Schweitzer-Stenner,*,‡ Thomas Measey,‡ Lazaros Kakalis,§ Frank Jordan,§ Silvia Pizzanelli,|| Claudia Forte,|| and Kai Griebenow⊥

Department of Chemistry, Drexel University, Philadelphia, Pennsylvania 19104, Department of Chemistry, Rutgers University, Newark, New Jersey 07102, Istituto per I Processi Chimico-Fisici, Consiglio Nazionale della Richerche, Area della Ricerca di Pisa via G. Moruzzi, 56124 Pisa, Italy, and Department of Chemistry, University of Puerto Rico, Río Piedras Campus, San Juan, Puerto Rico 09314

Received October 26, 2006; Revised Manuscript Received December 2, 2006

ABSTRACT: We have used a combination of FTIR, VCD, ECD, Raman, and NMR spectroscopies to probe the solution conformations sampled by H-(AAKA)-OH by utilizing an excitonic coupling model and constraints imposed by the $^3J_{C\alpha HNH}$ coupling constants of the central residues to simulate the amide I′ profile of the IR, isotropic Raman, anisotropic Raman, and VCD spectra in terms of a mixture of three conformations, i.e., polyproline II, β-strand and right-handed helical. The representative coordinates of the three conformations were obtained from published coil libraries. Alanine was found to exhibit PPII fractions of 0.60 or greater, mixed with smaller fractions of helices and β-strand conformations. Lysine showed no clear conformational propensity in that it samples polyproline II, β-strand, and helical conformations with comparable probability. This is at variance with results obtained earlier for ionized polylysine, which suggest a high polyproline II propensity. We reanalyzed previously investigated tetra- and trialanine by combining published vibrational spectroscopy data with $^3J_{C\alpha HNH}$ coupling constants and obtained again blends dominated by PPII with smaller admixtures of β-strand and right-handed helical conformations. The polyproline II propensity of alanine was found to be higher in tetraalanine than in trialanine. For all peptides investigated, our results rule out a substantial population of turn-like conformations. Our results are in excellent agreement with MD simulations on short alanine peptides by Gnanakaran and Garcia [(2003) *J. Phys. Chem. B 107*, 12555−12557] but at variance with multiple MD simulations particularly for the alanine dipeptide.

Alanine-based peptides have been the subject of intense research activities over the last 20 years. These were initiated by the discovery of Marquesee et al. that comparatively short polyalanine peptides with more than 12 residues doped with a limited number of charged residues can adopt an α-helical conformation in aqueous solution (*1*, *2*), in contrast to the conventional belief that only very long peptides can adopt this structure outside of the scaffold provided by the tertiary structure of a protein (*2*). These peptides continue to serve as convenient model systems for studying helix ↔ coil transitions (*3*, *4*).

More recently, the interest of the protein/peptide folding community has additionally focused on the unfolded state of alanine-based peptides, after theoretical and experimental results had suggested that it cannot be described by Tanford (*5*) and Flory's (*6*) classical random coil model. Shi et al. (*7*), for instance, used NMR and electronic CD (ECD)[1] measurements to study the structure of Ac-XX(A)$_7$OO-NH$_2$ (XAO, where X and O denote diaminobutyric acid and ornithine, respectively) and interpreted their results as indicating that the individual residues predominantly adopt a polyproline II (PPII) conformation at room temperature. The canonical PPII conformation is associated with the crystal structure of *trans*-polyproline (*8*) and exhibits dihedral angles of approximately (ϕ, ψ) = (−75°, 145°). The results of Shi et al. have been corroborated by numerous experimental and theoretical studies, which are indicative of a substantial PPII propensity of alanine (*9*−*12*), but were recently challenged by Scheraga, Liwo, and colleagues on the basis of a very comprehensive analysis of NMR and small angle scattering (SAXS) measurements on XAO (*13*). These authors concluded that PPII is one of many conformations sampled by alanine, thus reinforcing the validity of the statistical coil model (*5*, *6*, *14*). A predominance of PPII in the conformational manifold of XAO is also at odds with

† Financial support was provided from the NIH-COBRE II grant for the Center for Research in Protein Structure, Function, and Dynamics (P20 RR16439-01) and from the National Science Foundation (MCB-0318749).

* Corresponding author. Telephone: (215) 895-2268. Fax: (215) 895-1265. E-mail: RSchweitzer-Stenner@drexel.edu.

‡ Drexel University.

§ Rutgers University.

|| Consiglio Nazionale della Richerche.

⊥ University of Puerto Rico.

[1] Abbreviations: VCD, vibrational circular dichroism; ECD, electronic circular dichroism; PPII, poly(L-proline); MD, molecular dynamics; DFT, density functional theory.

10.1021/bi062224l CCC: $37.00
Published on Web 01/20/2007

the rather small radius of gyration inferred from SAXS measurements (*15*). Molecular dynamics simulations of the alanine dipeptide and polyalanines of varying lengths have increased the confusion in that different force fields yield rather different Ramachandran plots for the very same peptide. Some of these simulations support the high PPII propensity of alanine (*16*, *17*), while others do not even yield a substantial population of this conformation (*18*, *19*). Analyses of coil libraries seem to support a PPII preference of alanine, but this depends on how the data set is chosen (*20*). Even those simulations supporting the PPII propensity of alanine indicate an additional sampling of helix-like conformations, which is generally not considered in the analysis of experimental data (*23*, *26*).

In the current study we combine, for the first time, FTIR, polarized Raman, VCD (vibrational circular dichroism), ECD, and NMR data to explore the conformations of an alanine-based peptide, namely, the unblocked cationic tetrapeptide H-AAKA-OH (AAKA). We have chosen this peptide for two reasons. First, we aimed at obtaining the propensity of lysine as a guest in an alanine host system. Polylysine peptides of different lengths have been shown to prefer PPII (*21*, *22*), but for AKA, the conformation of K was found to depend on the C-terminal protonation state (*23*). This raises the question of whether lysine itself has a high PPII propensity, which is of relevance for the understanding of naturally unfolded proteins in which lysine residues occur much more frequently than in folded proteins (*24*). Second, lysine is one of the residues used in helix-forming alanine-based peptides, because it increases the overall helix stability, most likely by dehydrating the adjacent part of the backbone (*25*). We performed a structure analysis of AAKA by exploiting the excitonic coupling between the amide I′ modes of the three peptide groups, which produces conformationally sensitive IR, Raman, and VCD band profiles. For the simulation of the profiles we used a more extended approach than that employed for tri- and tetrapeptides in our earlier studies (*23*, *26*) by explicitly considering coexisting conformations for the individual residues. The statistical modeling was constrained by the $^3J_{C\alpha HNH}$ coupling constants of the residues obtained from ^{1}H NMR experiments. Subsequently, we utilized the same approach to reanalyze earlier published amide I′ band profiles of tetra- and trialanine, in conjunction with respective NMR data. The results led us to conclude a modified view about the conformational propensity of alanine, which is in excellent agreement with MD simulations of Gnanakaran and Garcia (*16*). With respect to lysine, our results show that it exhibits a reduced PPII propensity in an alanine context. Technically, the current study shows that the combination of NMR and vibrational spectroscopy provides a powerful tool to explore the conformational landscape of peptides.

MATERIALS AND METHODS

Materials. H-(Ala-Ala-Lys-Ala)-OH was custom synthesized by Celtek Peptides (Nashville, TN), with a purity of >98%. The peptide contained a small amount of TFA, which was removed by dialysis in a Spectra/Por CE Float-A-Lyzer bag, and the peptide was lyophilized overnight. For IR, VCD, and Raman measurements, the peptide was dissolved at a concentration of 0.1 M in 0.025 M $NaClO_4$ in D_2O (pD = 1), where the ClO_4^- Raman peak at 934 cm^{-1} was used as an internal standard (*27*) and the D_2O was made acidic by addition of DCl. Both D_2O and DCl were obtained from Sigma-Aldrich. After addition of the peptide, the solution had pD = 1.5.

L-Lysyl-L-alanine (KA) was purchased from Bachem Bioscience, Inc. (>96% purity). For the VCD measurement, the peptide was dissolved in D_2O at a concentration of 0.2 M (pD = 1.1).

Spectroscopies. The polarized Raman spectra were obtained with the 442 nm (32 mW) excitation from a HeCd laser (Model IK 4601R-E; Kimmon Electric US). The laser beam was directed into a RM 100 Renishaw confocal Raman microscope and focused onto a 1.0 mm Q silica cell with a thin glass cover slip using a 50× objective. The scattered light was filtered with a 442 nm notch filter, dispersed by a single-grating 2400 lines/mm grating, and imaged onto a back-thinned Wright Instrument CCD. It was polarized by a combination of a linear polarizer and a $\lambda/2$ plate. The latter rotates the *y*-polarized light (perpendicular to the laser polarization) into the *x*-direction to achieve an optimal spectrometer transmission. All spectra were recorded in the "continuous" mode. The peptide and the appropriate reference were measured a total of five times for each of the polarization directions, and the spectra were averaged to eliminate some of the noise. The reference spectra were appropriately subtracted from the sample spectra.

The FTIR and VCD spectra were recorded with a Chiral IR Fourier transform VCD spectrometer from Bio Tools. The sample was placed into a cell with a path length of 50 μm. The spectral resolution was 8 cm^{-1} for all measurements. The VCD and IR were both collected as one measurement for a combined total time of 720 min. To eliminate any background and solvent contributions to the IR spectrum, the cell was first filled with the reference solvent, i.e., acidic D_2O, which was automatically subtracted from the IR sample spectrum by the Chiral IR software.

Temperature-dependent ECD spectra were obtained using an OLIS DSM-10 UV/vis CD spectrophotometer. A 1.0 mm path length quartz cell was used, and the spectra were collected at 2 nm resolution. A peptide concentration of 1.0 mM in D_2O (pD = 1) was used. The sample was placed in a nitrogen-purged OLIS CD module. The sample temperature was controlled by means of a Peltier-type heating system (accuracy ±1 °C). Spectra were recorded from 20 to 80 °C at 10° intervals, averaging five scans at each temperature. The sample was allowed to equilibrate for 5 min at a given temperature. The spectra were collected as milliabsorbance as a function of wavelength and converted to molar absorptivities via Beer's law.

NMR samples of AAKA were prepared by dissolving the peptide at ca. 5 mM concentration in either D_2O (99.8 atom % D; Cambridge Isotope Laboratories) or a mixture of 90% H_2O/10% D_2O. One- and two-dimensional proton NMR spectra were acquired at 25 °C using a Varian INOVA NMR spectrometer (Varian Inc., Palo Alto, CA) operating at a proton frequency of 499.9 MHz and equipped with a 5 mm dual broad-band *z*-gradient probe.

Two-dimensional proton correlation spectroscopy, COSY (*28*, *29*), and NOE spectroscopy, NOESY (*30*, *31*), spectra were recorded in the pure absorption mode by employing the TPPI improvement (*32*, *33*) of the States−Haberkorn−Ruben hypercomplex method (*34*). Selection of desirable

Table 1: ^{1}H Chemical Shifts (ppm) of AAAA in Aqueous Solution at 0.025 M and Room Temperature[a]

residue no.	NH	CH^{α}	CH^{β}
1		4.01	1.46
2	8.53	4.27	1.34
3	8.36	4.22	1.32
4	7.88	4.04	1.26

[a] The proton chemical shifts are referenced to the water signal, which was set at 4.75 ppm.

coherences and artifact suppression were accomplished by *z*-gradients (COSY) and phase cycles of 4 (COSY) or 32 (NOESY) steps. The NOESY data set was acquired using a 600 ms mixing time. Typically, 256 t_1 increments of 2K complex data points over a 6 kHz spectral width were collected with 4 (COSY) or 32 (NOESY) scans per t_1 increment, preceded by 4 or 32 dummy scans, and a relaxation delay of 1.5 s. All spectra were acquired with the carrier offset placed on the water resonance, which was reduced by either solvent presaturation (*35*) or tailored excitation, using WATERGATE (*36*, *37*). The peptide NH resonances must not be in fast exchange with water since they were readily observed in 90% H_2O.

Data sets were processed on a Sun Blade 100 workstation (Sun Microsystems Inc., Palo Alto, CA) using the VNMR software package (Varian Inc., Palo Alto, CA). In order to decrease t_1 ridges arising from incorrect treatment of the first data point in the discrete Fourier transform (FT) algorithm, the spectrum corresponding to the first t_1 value was divided by 2 prior to FT along t_1 (*38*). Shifted (COSY) or unshifted (NOESY) Gaussian window functions were used in both dimensions. Data sets were zero-filled in the t_1 dimension, yielding 1K × 1K final matrices that have not been symmetrized. Spectra were referenced to the HDO resonance of the D_2O sample [4.76 ppm vs 4,4-dimethylsilapentane-sulfonic acid (deuterated at carbons 2 and 3) at 0.00 ppm].

The amino acid spin systems of AAKA were identified from the COSY spectra in D_2O and 90% H_2O/10% D_2O. The sequential assignments were made from the α CH_i−NH_{i+1} cross-peaks of the NOESY spectrum in 90% H_2O/10% D_2O (*39*). The $^3J_{C\alpha HNH}$ values were obtained from one-dimensional spectra of 32K complex data points over a 6 kHz spectral width.

^{1}H NMR experiments on AAAA (>98% purity; Bachem Bioscience Inc.) in aqueous solution (0.025 M) were performed at room temperature on a Bruker AMX-300 WB spectrometer equipped with a 5 mm reverse probe, using standard Bruker pulse programs. The $\pi/2$ pulse was 5.7 μs, and the relaxation delay was set to 4 s. The water signal was presaturated using a 4 s soft pulse (B_1 = 25 Hz). The assignment of the signals (Table 1) was performed through the cross-peaks of the ^{1}H DQF-COSY and NOESY experiments in the amide−H^{α} proton region (*39*), the former yielding the *J* connectivities and the latter allowing the identification of adjacent residues from the H^{α} and the amide proton of the subsequent residue cross-peak. The signal from the protons bound to the terminal nitrogen could not be identified because of their rapid exchange with water. The $^3J_{C\alpha HNH}$ coupling constants were obtained from the DQF-COSY experiment. NOESY experiments with mixing times ranging from 200 to 400 ms were acquired.

Spectral Analysis. All IR and Raman spectra were treated by using the program MULTIFIT (*40*). The calibration of the Raman spectrum was checked by using the $NaClO_4$ band at 934 cm^{-1}. To eliminate solvent contributions, we measured the solvent reference spectra for both polarizations, which were then subtracted from the corresponding peptide spectra. The isotropic and anisotropic Raman intensities were calculated as

$$I_{iso} = I_x - (4/3)I_y$$
$$I_{aniso} = I_y \quad (1)$$

where I_x and I_y denote the Raman scattering polarized parallel and perpendicular to the polarization of the exciting laser light.

RESULTS AND DISCUSSION

AAKA. The amide I′ band profiles of AAKA in D_2O as measured at acidic pD are displayed in Figure 1. This condition was chosen because it allows maximal spectral resolution and avoids the instabilities (i.e., precipitation) sometimes encountered at neutral pD. A comparison of the band profiles reveals a significant split between the peak positions of the isotropic Raman and the IR band profile. The anisotropic band has its peak between those of the IR and isotropic Raman band, but it is slightly closer to the IR band position. This is typical for a peptide with a predominant fraction of PPII (*41*−*43*). The respective VCD spectrum displays an asymmetric negative couplet with a large negative signal at the position of the lowest wavenumber amide I′ subband, which is predominantly assignable to the C-terminal peptide group (*44*). This negative signal reflects an intrinsic magnetic moment of this particular amide I′ mode, which gives rise to a negative Cotton effect, even in the spectrum of a dipeptide. This is illustrated by the amide I′ VCD spectrum of L-lysyl-L-alanine (KA) in Figure 2, which was also measured at acidic pD. The $^3J_{C\alpha HNH}$ coupling constants and the respective chemical shifts of residues 2−4 of AAKA are listed in Table 2.

We first analyzed the VCD spectrum of KA by using

$$\Delta\epsilon(\Omega) = \frac{\Omega_0 \,\mathrm{Im}(\vec{\mu}\cdot\vec{m})}{2.3 \times 10^{-39}\,\mathrm{M\cdot esu^2\,cm^2}} f(\Omega,\Omega_0) \quad (2)$$

where Ω_0 is the peak wavenumber of amide I′ and $\vec{\mu}$ the electronic and $\vec{m}$ the magnetic transition dipole moment. $f(\Omega,\Omega_0)$ denotes the Gaussian band profile. We used the electronic dipole moment of cationic KA reported by Measey et al. (*45*), a magnetic dipole moment of 2.3×10^{-23} esu cm, and an orientational angle of 10° for $\vec{m}$ with respect to the NC axis of the C-terminal residue (*46*). For $\vec{\mu}$, we used the orientational angle reported in earlier papers (*42*). The wavenumber and half-width were obtained from the respective IR band profile (data not shown). Thus, we obtained the fit of the VCD signal visualized by a solid line in Figure 2.

The excitonic coupling model for amide I has been described in detail in several earlier papers (*26*, *42*). It describes the amide I band profiles of IR, isotropic Raman, anisotropic Raman, and VCD in terms of nearest neighbor

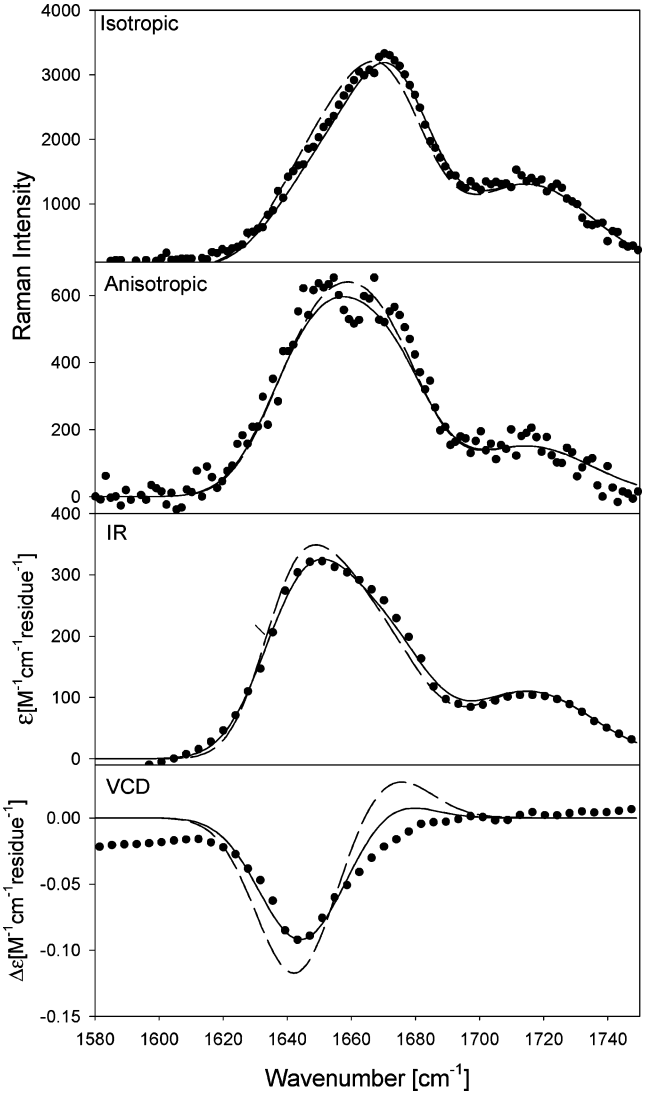

FIGURE 1: Amide I′ band profile (dotted) of the isotropic Raman, anisotropic Raman, IR, and VCD spectra of AAKA measured at pD = 1.5. The solid line results from a simulation based on a three-state (per residue) model, encompassing PPII, β, and helix-like conformations derived from the coil library of Avbelj and Baldwin (*48*) (PPII and β) and the MD simulations of Duan et al. (*17*) (helical). The dashed line was calculated with a two-state model (PPII and β). The band of the C-terminal carbonyl stretching mode has been modeled for the sake of completeness by fitting a Gaussian profile to the experimental data with the wavenumber and half-width as free parameters.

and non-nearest neighbor excitonic coupling between the excited states of the local oscillators (*47*) and the dihedral angles ϕ and ψ of the residues between the interacting amide I modes. We count the first central residue (starting at the N-terminal) as 1 and the subsequent one as 2. It should be noted that the two terminal residues are not probed by the amide I′ band profile.

Since each configuration of a peptide gives rise to an individual set of band profiles, the total intensity of a peptide ensemble is written as

$$I(\Omega) = \frac{\sum_{i=1}^{3}\sum_{j_1,j_2=1}^{n_{c_1},n_{c_2}} (I_{ij_1j_2}(\Omega)\mathrm{e}^{-(\Sigma_{k=1}^{2} G_{jk})/RT})}{Z} \qquad (3)$$

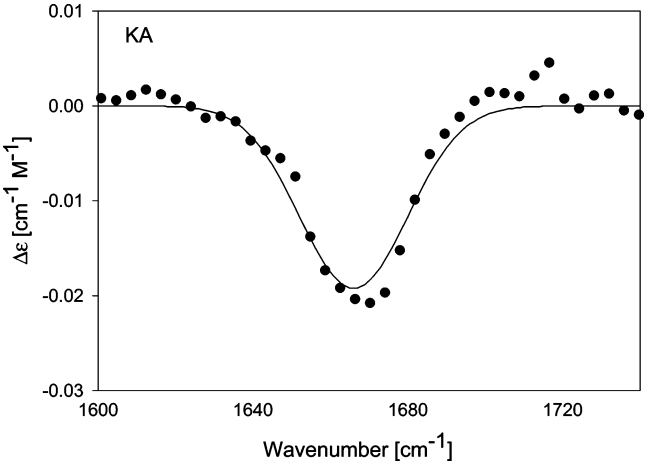

FIGURE 2: VCD spectrum of KA at pD = 1.5. The solid line results from a fit described in the text.

Table 2: $^3J_{C\alpha HNH}$ Values for AAKA

residue no.	$^3J_{\alpha HNH}$ (Hz)
2 (Ala)	5.18
3 (Lys)	6.46
4 (Ala)	6.72

where G_{j_k} is the Gibbs energy of the kth residue with the conformation j. The subscript i labels the excitonic state of the amide I′ oscillators. $I_{ij_1j_2}(\Omega)$ is thus the intensity profile of the ith excitonic state associated with the configuration $\{j_1,j_2\}$ of the tetrapeptide. R is the gas constant, T the absolute temperature, Z the partition sum of the ensemble, and n_{c_1} and n_{c_2} are the number of conformations considered for the two central residues.

In our analysis, we considered three representative conformations, i.e., PPII ($j = 1$), β ($j = 2$), and helical ($j = 3$). The Gibbs energy of PPII was set to zero. In a first step, we based our simulation on $(\phi, \psi)_1 = (-65°, 150°)$ and $(\phi, \psi)_2 = (-125°, 115°)$ for alanine, which represent respective distributions in the coil library of Avbelj and Baldwin (*48*) and correspond to the $^3J_{C\alpha HNH}$ constants reported by Shi et al. (*10*). For lysine, these authors reported a slightly different $^3J_{C\alpha HNH}$ value for PPII, which corresponds to $\phi = -68°$. Coil libraries as well as molecular dynamics simulations for alanine dipeptides generally exhibit helical distributions with a maximum at $(\phi, \psi)_3 = (-65°, 30°)$, which we assumed as representative for right-handed helical conformations (*17*). These coordinates are closer to a 3_{10} than to a canonical α-helical conformation (*49*). In the following, we refer to this structural model as the "coil library model".

We utilized the $^3J_{C\alpha HNH}$ constants of these conformations and our experimentally determined coupling constants to determine the mole fraction of the three considered conformations as follows:

$$\chi_{1,k} = \frac{(J_k - J_{\beta,k}) - \chi_{3,k}(J_\alpha - J_{\beta,k})}{J_{p,k} - J_{\beta,k}}$$

$$\chi_{2,k} = 1 - \chi_{1,k} - \chi_{3,k} \qquad (4)$$

where $\chi_{j,k}$ is the mole fraction of the kth residue in the jth conformation, J_k is the measured coupling constant of the kth residue, and $J_{p,k}$ and $J_{\beta,k}$ are the coil library coupling constants of the kth residue for PPII and β as reported by

Shi et al. (*10*). $J_\alpha = 4.1$ Hz is the representative coupling constant of the above helical conformation. The mole fraction $\chi_{3,k}$ of this conformation has been used as an adjustable parameter in the simulation. The mole fractions were used to calculate the relative Gibbs energies of the residues:

$$G_{j_k} = RT \ln(\chi_{j,k}/\chi_{1,k}) \quad (5)$$

which were used in eq 3 to calculate the intensity profiles.

We simulated the amide I′ band profiles of AAKA assuming solely a coexistence of PPII and β for each residue, i.e., $\chi_{3,k} = 0$. We did not consider any cooperativity, in accordance with the isolated pair hypothesis (*6*) and the temperature dependence of the ECD spectra reported below. The nearest neighbor coupling constants (5.0 for PPII and 2.5 for β) were taken from the ab initio study on a diglycine peptide by Torii and Tasumi (*50*). For PPII, this is in the interval of values observed earlier from isotropic Raman and femtosecond IR data of tripeptides (*44*, *46*). The respective β-strand value is slightly lower than that obtained for trivaline (*46*). The coupling between the N- and C-terminal amide I′ modes was calculated using the transition dipole formalism (*51*). We used MULTIFIT to self-consistently decompose the IR and Raman band profiles in Figure 1 into three bands as described in an earlier study (*25*) and used the thus obtained wavenumbers as a basis for guessing the wavenumber positions of the unperturbed amide I′ modes. The Gaussian bandwidths for the individual bands were also obtained from this analysis. Moreover, we used the recently reported electronic transition dipole moments of AA and KA (*45*). This yielded band profiles which reproduced the IR and Raman data reasonably well (dashed line in Figure 1), though some small deviations between simulated and experimental IR band profiles are notable. The VCD simulation, however, totally overestimated the large negative signal, which is much more pronounced than in the spectrum of KA. Additionally, it overestimated the positive signal at higher wavenumbers. A satisfactory simulation required a much larger magnetic transition dipole moment for the C-terminal amide I′ modes, i.e., 1.3×10^{-22} esu cm (dashed line in the lower panel of Figure 1). In a third step, we checked for the possibility that a small fraction of helical conformations are present in the sample. Indeed, we obtained a better agreement for the IR band profile, the highly asymmetric shape of which was nicely reproduced with a mole fraction of 0.3 for both residues (solid line in Figure 1). Larger values for $\chi_{3,k}$ yield substantial deviations from the experimental data in that too much intensity is accumulated at the highest wavenumber position, as expected for a predominantly helical band profile (*52*). We also checked the possibility that only one of the central residues adopts helical conformations, but that did not improve the profiles compared with the two-state (PPII/β) simulation. Thus, our final result yields PPII fractions of $\chi_{1,1} = 0.63$ for alanine and $\chi_{1,2} = 0.36$ for lysine, the β-fractions are $\chi_{2,1} = 0.07$ for alanine and $\chi_{2,2} = 0.34$ for lysine. Hence, alanine has a clear PPII propensity, but the values for lysine suggest a statistical coil behavior, in contrast to what has been observed for polylysine peptides (*21*, *22*, *53*).

Additionally, we considered slightly different representative structures for our three basic conformations. The band profiles of a simulation based on the PPII, β, and helix conformations in Figure 3 emerged from the MD simulation of Garcia, namely, $(\phi, \psi)_1 = (-60°, 120°)$, $(\phi, \psi)_2 = (-150°, 120°)$, and $(\phi, \psi)_3 = (-60°, 60°)$, respectively (*54*). The respective $^3J_{C\alpha HNH}$ constants were adjusted using the modified Karplus equation of Vuister and Bax (*55*). The representative PPII conformation resembles more the structure adopted by the first residue in a type II β-turn. The best reproduction of the experimental profiles was obtained with $\chi_{3,k} = 0.20$. The agreement between simulated and experimental profiles is not bad, but small systematic differences are discernible for IR, isotropic, and anisotropic Raman. The respective PPII fractions are $\chi_{1,1} = 0.60$ for alanine and $\chi_{1,2} = 0.45$ for lysine, while the β-fractions are $\chi_{2,1} = 0.19$ and $\chi_{2,2} = 0.35$ for alanine and lysine, respectively. Thus, alanine still has a clear PPII propensity. The respective value for lysine is slightly larger than that obtained from the coil library model.

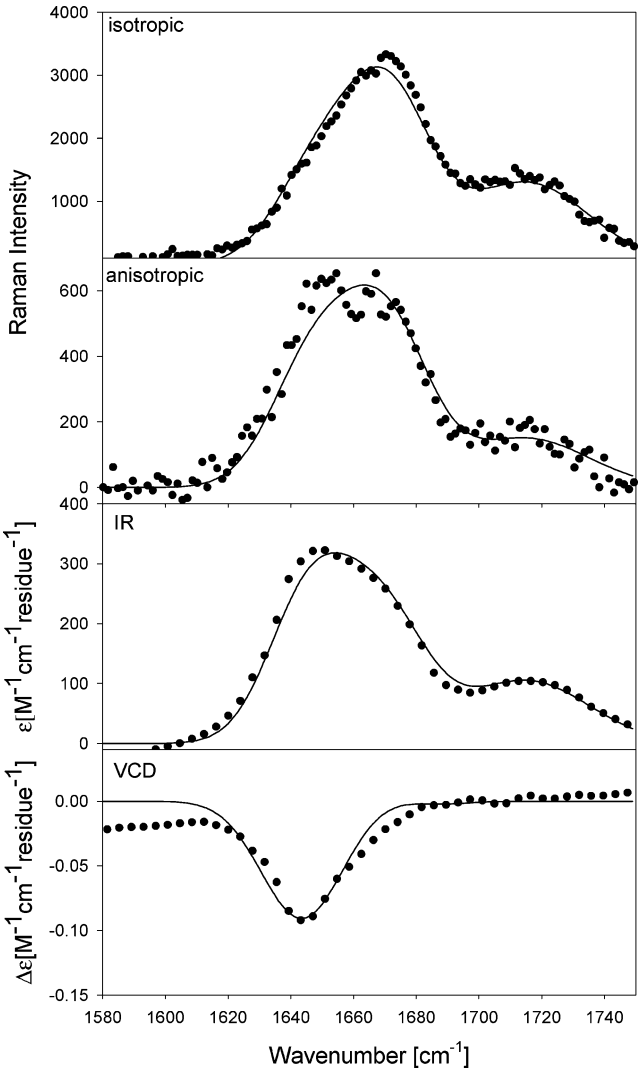

FIGURE 3: Amide I′ band profile (dotted) of the isotropic Raman, anisotropic Raman, IR, and VCD spectrum of AAKA measured at acidic pD 1. The solid line results from a simulation based on the three-state (per residue) model, encompassing PPII, β, and helix-like conformations derived from MD simulations of Gnanakaran and Garcia (*16*). The band of the C-terminal carbonyl stretching modes has been modeled for the sake of completeness by fitting a Gaussian profile to the experimental data with wavenumber and half-width as free parameters.

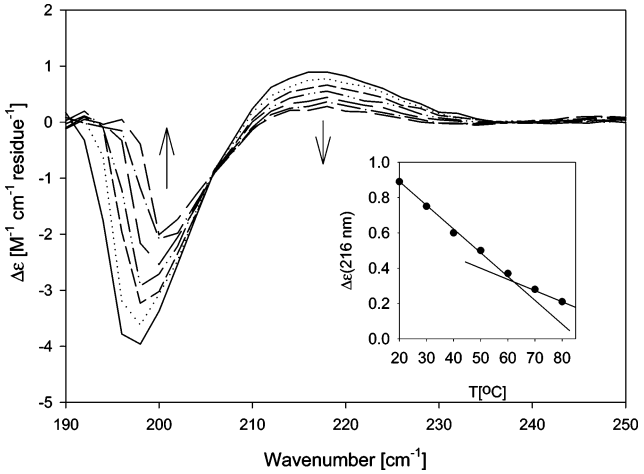

FIGURE 4: Temperature-dependent ECD spectra of AAKA at pD 1 measured from 20 to 80 °C at 10 deg intervals.

The temperature-dependent ECD spectra of AAKA plotted in units of M^{-1} cm^{-1} $residue^{-1}$ are depicted in Figure 4. In contrast to what has been obtained for the heavily debated XAO peptide, the spectra exhibit the characteristic minimum (195 nm) and maximum (215 nm) diagnostic of a substantial PPII contribution (*56*). However, compared with tetraalanine, both the maximum and minimum are reduced by a factor of 2 and 3, respectively (*26*). This is qualitatively in line with the much larger PPII fraction reported earlier for tetraalanine.

We wish to emphasize that the two sets of representative structures considered above are most likely part of a distribution of conformations assignable to different basins in the Ramachandran plot. The widths of these distributions are yet to be determined. Different coil libraries and results from MD simulations are far away from agreeing with each other with respect to the corresponding mole fractions and distribution widths of the sampled conformations. A classical random coil distribution of, e.g., alanine, as it emerged from the work of Ramachandran et al. (*57*) and Brant and Flory (*58*), can definitely be ruled out from our experimental data. We also considered the possibility of various turn conformations to contribute to the AAKA ensemble. The agreement with the experimental profiles was poor at best, even if only small fractions of, e.g., β-turns were considered.

Tetra- and Trialanine. In the past, we have used a somewhat less advanced model to determine the average structure of tri- and tetrapeptides, in that we identified the dihedral angles which reproduced the intensity ratios of the individual amide I′ subbands derived from spectral decomposition. The result was subsequently interpreted in terms of a two-state model, solely considering PPII and an extended β-strand conformation, which is different from the more parallel β-sheet-like dihedral angles used in the present study. Therefore, we felt a necessity to reanalyze both tetra- and trialanine by means of our statistical model. The earlier reported band profiles of (cationic) tetraalanine and (zwitterionic) trialanine are depicted in Figures 5 and 6, respectively. Additionally, we measured the $^3J_{C\alpha HNH}$ coupling constants for tetraalanine; these values are listed in Table 3, while the coupling constant for the central alanine residue in AAA (i.e., 5.6 Hz) was obtained from Schwalbe, Stock, and associates (*73*). Again, we used these constants to restrict the simulations of the band profiles by means of eq 4. In a

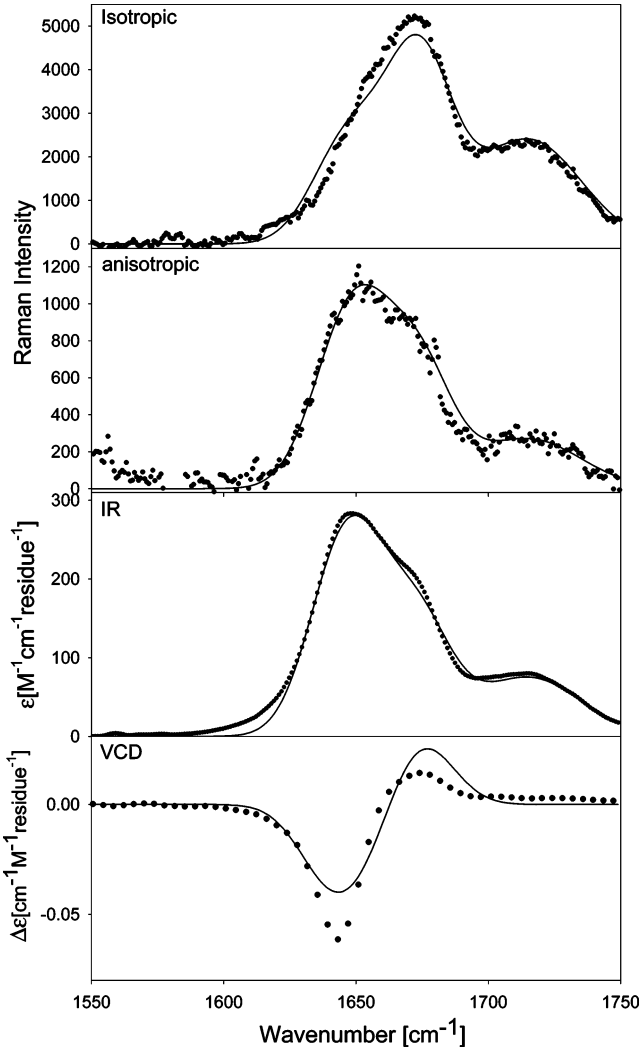

FIGURE 5: Amide I′ band profile of the isotropic Raman, anisotropic Raman, IR, and VCD spectrum of AAAA measured at acidic pD 1 (taken from ref *26*). The solid line results from a simulation based on a three-state (per residue) model, encompassing PPII, β, and helix-like conformations as described in the text. The band of the C-terminal carbonyl stretching modes has been modeled for the sake of completeness by fitting a Gaussian profile to the experimental data with wavenumber and half-width as free parameters.

first step, we considered the representative conformations of the coil library model and obtained an insufficient agreement with the experimental data, irrespective of our choice of the helical fraction. That particularly concerned the IR and anisotropic Raman band profiles, for which the relatively large intensity of the lowest wavenumber band could not be reproduced. For tetraalanine, however, we could obtain a rather good agreement with the experimental profiles by using the representative conformation obtained in our earlier study (with ϕ angles of $-70°$ and $-80°$), but this is not consistent with the observed $^3J_{C\alpha HNH}$ coupling constants listed in Table 3. Inclusion of any of the different types of turns in the simulation led to poorer agreement with the experimental data. Subsequently, we decided to modify the coordinates of the representative PPII conformations and finally obtained the simulation in Figure 5 for tetraalanine, by assuming that the difference between the $^3J_{C\alpha HNH}$ coupling constants reflects different PPII coordinates rather than different conformational mixtures. The agreement with the

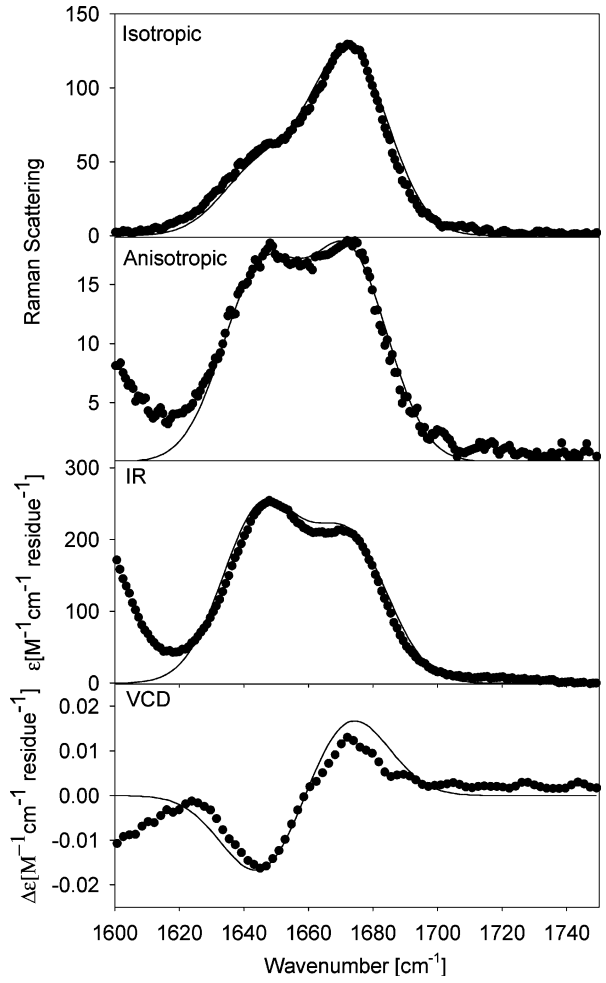

FIGURE 6: Amide I′ band profile of the isotropic Raman, anisotropic Raman, IR, and VCD spectrum of AAA measured at neutral pD 6 (taken from ref *34*). The solid line results from a simulation based on a three-state (per residue) model, encompassing PPII, β, and helix-like conformations as described in the text.

Table 3: $^3J_{C\alpha HNH}$ Values for Tetraalanine (AAAA)

residue no.	$^3J_{\alpha HNH}$ (Hz)
2	5.50
3	6.03
4	6.92

experimental data can be considered as satisfactory. The respective PPII conformations are $(\phi, \psi)_{11} = (-65°, 150°)$ and $(\phi, \psi)_{12} = (-70°, 140°)$. Helical contributions had to be considered, and we obtained different fractions for the two residues, namely, $\chi_{3,1} = 0.20$ for the first and $\chi_{3,2} = 0.10$ for the second of the nonterminal alanines (counted from the N-terminal). The PPII mole fractions are $\chi_{1,1} = 0.66$ and $\chi_{1,2} = 0.73$, while the β-fractions are $\chi_{2,1} = 0.14$ and $\chi_{2,2} = 0.17$. With respect to PPII, this is less than what was estimated in our earlier study, but the result still corroborates the notion that alanine has a high PPII propensity, contrary to recent claims (*13*). Additionally, we simulated the profiles with the coordinates representing the distributions of Gnanakaran and Garcia (*16*), but this did not reproduce any of the experimental profiles.

For tetraalanine, NOESY cross-peaks are observed in the H^N-H^α, H^N-H^{Me}, and $H^\alpha-H^{Me}$ regions, the first one being the most relevant for conformational analysis. In fact, as far as the internal residues are concerned, the H^N-H^α intraresidue cross-peaks are much less intense than the interresidue ones, suggesting that the latter are characterized by φ, ψ angles in the PPII and/or in the β-sheet Ramachandran region, for which $d_{H^{\alpha i}H^{N(i+1)}}$ distances are shorter than $d_{H^{\alpha i}H^{Ni}}$ (*17*). Moreover, the absence of measurable NOE's in the amide−amide region excludes the presence of appreciable amounts of α-helix conformers. These results corroborate in general terms the analysis of the vibrational spectra.

With respect to trialanine, Eker et al. reported a 50:50 mixture of PPII and β (*46*). This result cannot be brought in line with the $^3J_{C\alpha HNH}$ coupling constant of 5.6 Hz, however. The rather satisfactory simulation depicted in Figure 6 was obtained with the PPII conformation obtained from the coil library, namely, $(\phi, \psi)_{11} = (-68°, 150°)$. This PPII conformation is very close to the values reported in the early study of Woutersen and Hamm (*44*). The helical fraction of $\chi_3 = 0.25$ is a necessity. The respective PPII and β fractions are $\chi_1 = 0.52$ and $\chi_2 = 0.23$. Again, we also tried to simulate the profiles with the coordinates representing the distributions of Gnanakaran and Garcia (*16*), but the result was less satisfactory.

It is noteworthy that the C-terminal $^3J_{C\alpha HNH}$ coupling constants of AAKA and AAAA (6.7 and 6.9 Hz) are slightly higher than the respective value obtained for AA (6.5 Hz) (*59*), and all these values are higher than those of the central residues of the investigated peptides. We interpret this as indicating that terminal residues are more likely to sample β-strand-like conformations, which yield an increase of $^3J_{C\alpha HNH}$. If one invokes the two-state coupling model of Shi et al. (*10*) and the $^3J_{C\alpha HNH}$ constants of Avbelj and Baldwin (*48*), all of the values are still indicative of a high percentage of polyproline II, as argued by Dragomir et al. (*60*).

All of these analyses together demonstrate that the combination of our vibrational spectroscopy approach with NMR data (i.e., $^3J_{C\alpha HNH}$) is very powerful in identifying the conformational manifold of amino acid residues in peptides. This strategy takes advantage of the site-specific information provided by NMR, along with the high sensitivity of the amide I band profiles concerning even modest variations of the secondary structure. In this context, we would like to emphasize that this stems in part from the fact that second nearest neighbor coupling (i, $i + 2$) is not insignificant, particularly for the helical and the β-conformation.

Comparison with Literature. As mentioned above, the ECD spectra of various unfolded alanine-based peptides exhibit the characteristic feature indicative of a substantial fraction of PPII (*21*). The much discussed XAO peptide is somewhat of an exception from the rule in that its maximum at 216 nm is substantially reduced, which suggests the presence of other conformers (*52*). This and other experimental data for this particular peptide led Makowska et al. (*13*) and Vila et al. (*61*) to the conclusion that alanine does not have a substantial PPII propensity. The results of the present study strongly corroborate the opposite notion. The mole fraction of alanine was found to vary between 0.60 and 0.75 for the peptides investigated. These values are somewhat lower than those reported by Shi et al. for XAO (*10*), but still large enough to consider a PPII preference of alanine. Our analysis also corroborates the notion that the individual PPII propensity of alanine is higher in AAAA than in AAA (and AA (*59*)), in line with theoretical predictions

of Garcia (*54*) and Raman optical activity data reported by McColl (*12*).

The sampling of helical conformations by alanine in short peptides has been a matter of debate. Thus far, it has been overlooked in the studies of Kallenbach, Schweitzer-Stenner, and their respective associates. MD simulations, however, generally reveal a sampling of the helical basin of the Ramachandran plot (mostly right-handed), but the respective fraction does depend strongly on the choice of the force field (*19*). Woutersen et al. investigated the spectral broadening of the amide band I of trialanine and arrived at the conclusion that their sample of AAA contained 20% α_R and 80% PPII (*62*). Our own analysis for this peptide yields the same helical fraction, but a lower PPII propensity. The mixture reported by Woutersen et al. would be inconsistent with our amide I′ profiles and ECD data. Mu and Stock (*63*) performed MD simulations with a GROMOS 43A1 force field and obtained $\chi_1 = 0.41$ (PPII), $\chi_2 = 0.41$ (β), and $\chi_3 = 0.16$ (helical) for the central residue. This is close to our earlier reported 50:50 mixing of PPII and β but, as argued above, inconsistent with the $^3J_{C\alpha HNH}$ coupling constant. Duan et al. (*17*) used the force field of Cornell et al. (*64*) to carry out an MD simulation for an alanine dipeptide and a blocked alanine tetrapeptide in explicit water. For the dipeptide they obtained comparable populations of PPII and the (right-handed) helical fraction with a minor population of β. For the tetrapeptide, these three basins are nearly equally populated, so that their plot looks like the classical random coil distribution, which Ramachandran et al. (*57*) and Brant and Flory (*58*) obtained for the alanine dipeptide. All of these results are inconsistent with our experimental data. The discrepancy is even more pronounced for simulations which Hu et al. (*65*) and Zagrovic et al. (*15*) performed with different AMBER, CHARM, and GROMOS force fields for an alanine dipeptide and XAO, respectively. Kentsis et al. used a CHARM27 force field to calculate the propensities of all natural amino acids in GGXGG peptides (*9*). The so estimated alanine propensity for PPII is too low (30%). All of these simulations yield an overestimation of the helical fraction and an underestimation of PPII. Tran et al. used their own potential function and Monte Carlo simulations to obtain a mixture of nearly 50% PPII, 30% β (i.e., with angles of a parallel β-sheet), and approximately 18% helical conformations (*66*). This is closer to our results, but their PPII fraction contains a substantial amount of a conformation termed P_{hyp}, which exhibits lower ψ and ϕ values than the canonical PPII. Such conformations would exhibit a very low level of excitonic coupling for amide I (*50*) and are therefore not likely to contribute significantly to the observed amide I band profiles. Gnanakaran and Garcia used a modified AMBER force field (A94/MOD) to simulate the sampling of polyalanine peptides of different length (*16*). For the alanine dipeptide they observed a mixture of $\chi_1 = 0.59$ (PPII), $\chi_2 = 0.14$ (β), and $\chi_3 = 0.20$ (helical); for AAA they observed $\chi_1 = 0.80$ (PPII), $\chi_2 \approx 0.08$ (β), and $\chi_3 \approx 0.08$ (helical). Their result for the alanine dipeptide is very close to what we observed for the central residue of AAA, but even their result for AAAA is much closer to ours than all of the other simulations discussed above. Finally, it deserves to be mentioned that our results are in very good agreement with the PPII, β, and helix population of alanine in the (reduced) coil library of Serrano (*20*), but inconsistent with those in the respective library of Fiebig et al. (*67*).

We would also like to note the remarkable similarity between the dihedral angles which were used in the current study to simulate the vibrational spectra of tetraalanine and those reported recently by Pizzanelli et al. (*68*). The authors performed a DFT calculation for tetraalanine in implicit and explicit solvent (14 water molecules). The most stable conformation obtained was clearly PPII-like; the respective coordinates are $(\phi, \psi)_{11} = (-57.6°, 145.0°)$ and $(\phi, \psi)_{12} = (-68.8°, 138.4°)$ for the central residues. This is not only close to the values obtained in the present study but also reproduces the small difference between the two PPII conformations of the central residues, which we inferred from our data. The predominance of PPII was then confirmed by ^{1}H NMR spectroscopy by measuring the dipolar couplings of tetraalanine in an oriented lyotropic liquid crystal. The DFT calculations revealed a conformation with both residues in a helical conformation as the second one in the conformational hierarchy. The close resemblance between these values and those which we report affirms the merit of our current model, as well as supports the PPII propensity of alanine.

The low PPII propensity observed for the lysine residue in AAKA is somewhat surprising since earlier studies on charged polylysine peptides of different lengths were all in agreement in suggesting a high PPII propensity (*21*, *22*, *53*). That this property might depend on the choice of the nearest neighbors has already been indicated by Eker et al., who showed that K in AKA adopts β-strand-like conformations at neutral pD, whereas PPII is preferred at acidic conditions (*23*). More recently, Measey and Schweitzer-Stenner showed that the average PPII fraction of the octapeptide, $(AAKA)_2$, is 60%, which is lower than expected (*69*). We investigated AAKA at acidic conditions and showed that K samples PPII, β, and helical conformations. This seems to resemble the statistical coil concept of Zimmerman and Scheraga (*14*). The reason for this behavior might be that lysine perturbs the order of the hydration shell which has been suggested to stabilize PPII in polyalanine peptides (*70*). Generally, our result shows that nearest neighbor effects are relevant for individual propensities of amino acid residues, and that a PPII preferring neighbor does not necessarily support the PPII propensity of a given residue.

Taken together, our study provides compelling evidence for a significant PPII propensity of alanine, while it reveals a context-dependent behavior for lysine, which deserves further investigations. Furthermore, we showed that alanine samples, to some extent, also (right-handed) helical conformations, in line with predictions of Gnanakaran and Garcia (*16*), Mu and Stock (*63*), and Woutersen et al. (*62*). We would like to emphasize, however, that our results do not argue in favor of a somewhat simplistic notion that *the* structure of unfolded alanine peptides is PPII, as implicitly suggested in a recent paper by Asher et al. (*71*). If the individual PPII mole fraction of alanine is as high as 0.73 (as obtained for AAAA), the molar fraction of XAO with all alanines in PPII is 0.11. The corresponding fractions for six, five, and four residues are 0.08, 0.095, and 0.12, respectively. Thus, nearly 40% of the peptides exhibit PPII sequences of six and more. This is not insignificant. One has to take into account, however, that conformational

fluctuations are significant on the PPII potential surface; i.e., a PPII segment is still a dynamic entity. Nevertheless, it is justified to state that the classical random coil, or even the statistical coil, concept does not apply to alanine, and evidence exists that it does not apply to other types of residues either (*20*, *72*). With respect to XAO, which is currently being investigated in our laboratory, we have evidence for the notion that (in agreement with Makowska et al. (*13*)) turns can be formed at the interface between the alanine segment and the X_2 and O_2 segments at the termini, whereas the remaining alanine residues maintain a substantial PPII fraction (Schweitzer-Stenner and Measey, manuscript in preparation).

ACKNOWLEDGMENT

We thank Drs. Schwalbe and Stock for providing us with a preprint of their article (ref *73*), as well as some very useful discussions.

REFERENCES

1. Marqusee, S., and Baldwin, R. L. (1987) Helix stabilization by $Glu^{-}\cdots Lys^{+}$ salt bridges in short peptides of de novo design, *Proc. Natl. Acad. Sci. U.S.A. 84*, 8898−8902.
2. Scholtz, J. M., Marqusee, S., Baldwin, R. L., York, E. J., Stewart, J. M., Santoro, M., and Bolen. D. W. (1991) Calorimetric determination of the enthalpy change for the alpha-helix to coil transition of an alanine peptide in water, *Proc. Natl. Acad. Sci. U.S.A. 88*, 2854−2860.
3. Scholtz, J. M., and Baldwin, R. L. (1992) The mechanism of alpha-helix formation by peptides, *Annu. Rev. Biophys. Biomol. Struct. 21*, 95−118.
4. Lednev, I. K., Karnoup, A. S., Sparrow, M. C., and Asher, S. A. (1999) R-Helix peptide folding and unfolding activation barriers: A nanosecond UV resonance Raman study, *J. Am. Chem. Soc. 121*, 8074−8086.
5. Tanford, C. (1998) Protein denaturation, *Adv. Protein Chem. 23*, 121−282.
6. Flory, P. J. (1969) *Statistical Mechanics of Chain Molecules*, Wiley, New York.
7. Shi, Z., Olson, C. A., Rose, G. D., Baldwin, R. L., and Kallenbach, N. R. (2002) Polyproline II structure in a sequence of seven alanine residues, *Proc. Natl. Acad. Sci. U.S.A. 99*, 9190−9195.
8. Cowan, P. M., and McGavin, S. (1955) Structure of poly-L-proline, *Nature 176*, 501−503.
9. Kentsis, A., Mezei, M., and Osman, R. (2005) Origin of the sequence dependent polyproline II structure in unfolded proteins, *Proteins 61*, 769−776.
10. Shi, Z., Olson, C. A., Rose, G. A., Baldwin, R. L., and Kallenbach, N. R. (2005) Polyproline II propensities from GGXGG peptides reveal an anticorrelation with β-sheet scales, *Proc. Natl. Acad. Sci. U.S.A. 102*, 17964−17968.
11. Kelly, M. A., Chellgren, B. W., Rucker, A. L., Troutman, J. M., Fried, M. G., Miller, A., and Creamer, T. P. (2001) Host-guest study of left handed polyproline II helix formation, *Biochemistry 40*, 14376−14383.
12. McColl, I. H., Blanch, E. W., Hecht, L., Kalenbach, N. R., and Barron, L. D. (2004) Vibrational Raman optical activity characterization of poly(L-proline II) helix in alanine oligopeptides, *J. Am. Chem. Soc. 126*, 5076−5077.
13. Makowska, J., Rodziewicz-Motowidło, S., Bagińska, K., Vila, J. A., Liwo, A., Chmurzyński, L., and Scheraga, H. A. (2006) Polyproline II conformation is one of many local conformational states and is not an overall conformation of unfolded peptides and proteins, *Proc. Natl. Acad. Sci. U.S.A. 103*, 1744−1749.
14. Zimmermann, S. S., Pottle, M. S., Nèmethy, G., and Scheraga, H. A. (1976) Conformational analysis of the 20 naturally occurring amino acid residues using ECEPP, *Macromolecules 9*, 408−416.
15. Zagrovic, B., Lipfert, J., Sorin, E. J., Millett, I. S., van Gunsteren, W. F., Doniach, S., and Pande, V. S. (2005) Unusual compactness of a polyproline II structure, *Proc. Natl. Acad. Sci. U.S.A. 102*, 11698−11703.
16. Gnanakaran, S., and Garcia, A. (2003) Validation of an all-atom protein force field: from dipeptides to larger peptides, *J. Phys. Chem. B 107*, 12555−12557.
17. Duan, Y., Wu, C., Chowdhury, S., Lee, M. C., Xiong, G., Zhang, W., Yang, R., Cieplak, P., Luo, R., Lee, T., Caldwell, J., Wang, J., and Kollman, P. (2003) A point-charge force field for molecular mechanics simulations of proteins based on condensed-phase quantum mechanical calculations, *J. Comput. Chem. 24*, 1999−2012.
18. Gnanakaran, S., and Hochstrasser, R. M. (2001) Conformational preferences and vibrational frequency distributions of short peptides in relation to multidimensional infrared spectroscopy, *J. Am. Chem. Soc. 123*, 12886−12898.
19. Gnanakarna, S., and Garcia, A. E. (2005) Helix-coil transition of alanine peptides in water: Force field dependence on the folded and unfolded structures, *Proteins 59*, 773−782.
20. Serrano, L. (1995) Comparison between the ϕ-distribution of the amino acids in the Protein Data Base and NMR data indicates that amino acids have various ϕ propensities in the random coil conformation, *J. Mol. Biol. 254*, 322−333.
21. Tiffany, M. L., and Krimm, S. (1968) New chain conformations of poly(glutamic acid) and polylysine, *Biopolymers 6*, 1379−1382.
22. Rucker, A. L., and Creamer, T. P. (2002) Polyproline II helical structure in protein unfolded states: Lysine peptides revisited, *Protein Sci. 11*, 980−985.
23. Eker, F., Griebenow, K., Cao, X., Nafie, L. A., and Schweitzer-Stenner, R. (2004) Preferred backbone conformations in the unfolded state revealed by the structure analysis of alanine based (AXA) tripeptides in solution, *Proc. Natl. Acad. Sci. U.S.A. 101*, 10054−10059.
24. Tompa, P. (2002) Intrinsically unstructured proteins, *Trends Biochem. Sci. 27*, 527−533.
25. Vila, J. A., Ripoll, D. R., and Scheraga, H. A. (2001) Influence of lysine content and pH on the stability of alanine-based copolypeptide, *Biopolymers 58*, 235−246.
26. Schweitzer-Stenner, R., Eker, F., Griebenow, K., Cao, X., and Nafie, L. A. (2004) The conformation of tetraalanine in water determined by polarized Raman, FTIR and VCD spectroscopy, *J. Am. Chem. Soc. 126*, 2768−2776.
27. Sieler, G., and Schweitzer-Stenner, R. (1997) The amide I mode of peptides in aqueous solution involves vibrational coupling between the peptide group and water molecules of the hydration shell, *J. Am. Chem. Soc. 119*, 1720−1726.
28. Aue, W. P., Bartholdi, E., and Ernst, R. R. (1976) Two-dimensional spectroscopy. Application to nuclear magnetic resonance, *J. Chem. Phys. 64*, 2229−2246.
29. Bax, A., and Freeman, R. (1981) Investigation of complex networks of spin-spin coupling by two-dimensional NMR, *J. Magn. Reson. 44*, 542−561.
30. Jeener, J., Meier, B. H., Bachmann, P., and Ernst, R. R. (1979) Investigation of exchange processes by two-dimensional NMR spectroscopy, *J. Chem. Phys. 71*, 4546−4553.
31. Macura, S., and Ernst, R. R. (1980) Elucidation of cross relaxation in liquids by two-dimensional N.M.R. spectroscopy, *Mol. Phys. 41*, 95−117.
32. Redfield, A. G., and Kunz, S. D. (1975) Quadrature Fourier NMR detection: Simple multiplex for dual detection and discussion, *J. Magn. Reson. 19*, 250−254.
33. Marion, D., and Wüthrich, K. (1983) Application of phase sensitive two-dimensional correlated spectroscopy (COSY) for measurements of ^{1}H-^{1}H spin-spin coupling constants in proteins, *Biochem. Biophys. Res. Commun. 113*, 967−974.
34. States, D. J., Haberkorn, R. A., and Ruben, D. J. (1982) A two-dimensional nuclear overhauser experiment with pure absorption phase in four quadrants, *J. Magn. Reson. 48*, 286−292.
35. Hoult, D. I. (1976) Solvent peak saturation with single phase and quadrature fourier transformation, *J. Magn. Reson. 21*, 337−347.
36. Piotto, M., Saudek, V., and Sklenar, V. (1992) Gradient-tailored excitation for single-quantum. a. NMR spectroscopy of aqueous solutions, *J. Biomol. NMR 2*, 661−665.
37. Sklenar, V., Piotto, M., Leppik, R., and Saudek, V. (1993) Gradient-tailored water suppresion for H1-N15. HSQC experiments optimized to retain full sensitivity, *J. Magn. Reson. A 102*, 241−245.
38. Otting, G., Widmer, H., Wagner, G., and Wüthrich, K. (1986) Origin of τ_1 and τ_2 ridges in 2D a: NMR spectra and procedures for suppression, *J. Magn. Reson. 66*, 187−193.
39. Wüthrich, K. (1986) *NMR of Proteins and Nucleic Acids*, Wiley-Interscience, New York.

40. Jentzen, W., Unger, E., Karvounis, G., Shelnutt, J. A., Dreybrodt, W., and Schweitzer-Stenner, R. (1996) Conformational properties of nickel(II) octaethylporphyrin in solution. 1. Resonance excitation profiles and temperature dependence of structure-sensitive Raman lines, *J. Phys. Chem. 100*, 14184−14191.
41. Measey, T., and Schweitzer-Stenner, R. (2005) Simulation of amide I′ band profiles of trans polyproline based on an excitonic coupling model, *Chem. Phys. Lett. 408*, 123−127.
42. Schweitzer-Stenner, R. (2004) Secondary structure analysis of polypeptides based on an excitonic coupling model to describe the band profile of amide I of IR, Raman and vibrational circular dichroism spectra, *J. Phys. Chem. B 108*, 16965−16975.
43. Eker, F., Griebenow, K., and Schweitzer-Stenner, R. (2004) Aβ_{1-28} fragment of the amyloid peptide predominantly adopts a polyproline II conformation in an acidic solution, *Biochemistry 43*, 6893−6898.
44. Woutersen, S., and Hamm, P. (2000) Structure determination of trialanine in water using polarized sensitive two-dimensional vibrational spectroscopy, *J. Phys. Chem. B 104*, 11316−11320.
45. Measey, T., Hagarman, A., Eker, F., Griebenow, K., and Schweitzer-Stenner, R. (2005) Side chain dependence of intensity and wavenumber position of amide I′ in IR and visible Raman spectra of XA and AX dipeptides, *J. Phys. Chem. B 109*, 8195−8205.
46. Eker, F., Cao, X., Nafie, L., and Schweitzer-Stenner, R. (2002) Tripeptides adopt stable structures in water. A combined polarized visible Raman, FTIR and VCD spectroscopy study, *J. Am. Chem. Soc. 124*, 14330−14341.
47. Hamm, P., Lim, M., and Hochstrasser, R. (1998) Structure of the amide I band of peptides measured by femtosecond nonlinear-infrared spectroscopy, *J. Phys. Chem. B 102*, 6123−6138.
48. Avbelj, F., and Baldwin, R. L. (2003) Role of backbone solvation and electrostatics in generating preferred peptide backbone conformations: Distributions of ϕ, *Proc. Natl. Acad. Sci. U.S.A. 100*, 5742−5747.
49. Huggins, M. L. (1943) The structure of fibrous proteins, *Chem. Rev. 32*, 195−218.
50. Torii, H., and Tasumi, M. (1998) *Ab Initio* molecular orbital study of the amide I vibrational interactions between the peptide groups in di- and tripeptides and considerations on the conformation of the extended helix, *J. Raman Spectrosc. 29*, 81−86.
51. Krimm, S., and Badekar, J. (1986) Vibrational spectroscopy or peptides and proteins, *Adv. Protein Chem. 38*, 181−363.
52. Schweitzer-Stenner, R., Measey, T., Hagarman, A., Eker, F., and Griebenow, K. (2006) Salmon calcitonin and amyloid beta: Two peptides with amyloidogenic capacity adopt different conformational manifolds in their unfolded states, *Biochemistry 45*, 2810−2819.
53. Eker, F., Griebenow, K., Cao, X., Nafie, L., and Schweitzer-Stenner, R. (2004) Tripeptides with ionizable side chains adopt a perturbed polyproline II structure in water, *Biochemistry 43*, 613−621.
54. Garcia, A. (2004) Characterization of non-alpha conformations in Ala peptides, *Polymer 45*, 669−676.
55. Vuister, G. W., and Bax, A. (1993) Quantitative *J* correlation: a new approach for measuring homonuclear three-bond *J* (HN Ha) coupling, *J. Am. Chem. Soc. 115*, 7772−7777.
56. Sreerama, N., and Woody, R. W. (1994) Poly(Pro)II helices in globular proteins: identification and circular dichroic analysis, *Biochemistry 33*, 10022−10025.
57. Ramachandran, G. N., Ramakrishnan, C., and Sasisekharan, V. (1963) Stereochemistry of polypeptide chain configurations, *J. Mol. Biol. 7*, 95−99.
58. Brant, D. A., and Flory, P. J. (1965) The configuration of random polypeptide chains. II. Theory, *J. Am. Chem. Soc. 87*, 2791−2800.
59. Hagarman, A., Measey, T., Doddasomayajula, R. S., Dragomir, S., Eker, F., Griebenow, K., and Schweitzer-Stenner, R. (2006) Conformational analysis of XA and AX dipeptides in water by electronic circular spectroscopy, *J. Phys. Chem. B 110*, 6979−6986.
60. Dragomir, I., Measey, T. J., Hagarman, A. M., and Schweitzer-Stenner, R. (2006) Environment-controlled interchromophore charge transfer transitions in dipeptides probed by UV absorption and electronic circular dichroism spectroscopy, *J. Phys. Chem. B 110*, 13235−13241.
61. Vila, J. A., Baldoni, H. A., Ripoll, D. R., Ghosh, A., and Scheraga, H. A. (2004) Polyproline II helix conformation in a proline-rich environment: A theoretical study, *Biophys. J. 86*, 731−742.
62. Woutersen, S., Pfister, R., Hamm, P., Mu, Y., Kosov, D. S., and Stock, G. (2002) Peptide conformational heterogeneity revealed from nonlinear vibrational spectroscopy and molecular dynamics simulations, *J. Chem. Phys. 117*, 6833−6840.
63. Mu, Y., and Stock, G. (2002) Conformational dynamics of trialanine in water: A water dynamics study, *J. Phys. Chem. B 106*, 5294−5301.
64. Cornell, W. D., Cieplak, P., Bayly, C. I., Gould, I. R., Merz, K. M., Jr., Ferguson, D. M., Spellmeyer, D. C., Fox, T., Caldwell, J. W., and Kollman, P. A. (1995) A second generation force field for the simulation of proteins, nucleic acids, and organic molecules, *J. Am. Chem. Soc. 117*, 5179−5197.
65. Hu, H., Elstner, M., and Hermans, J. (2003) Comparison of a QM/MM force field and molecular mechanics force fields in simulations of alanine and glycine "dipeptides" (Ace-Ala-Nme and Ace-Gly-Nme) in water in relation to the problem of modeling the unfolded peptide backbone in solution, *Proteins 50*, 451−463.
66. Tran, H. T., Wang, X., and Pappu, R. V. (2005) Reconciling observations of sequence-specific conformational propensities with the generic polymeric behavior of denatured proteins, *Biochemistry 44*, 11369−11380.
67. Fiebig, K. M., Schwalbe, H., Buck, M., Smith, L. J., and Dobson, C. M. (1996) Toward a description of the conformations of denatured states of proteins, comparison of a random coil model with NMR measurements, *J. Phys. Chem. B 100*, 2661−2666.
68. Pizzanelli, S., Monti, S., and Forte, C. (2005) Conformation and orientation of tetralanine in a lyotropic liquid crystal studied by nuclear magnetic resonance, *J. Phys. Chem. B 109*, 21102−21109.
69. Measey, T., and Schweitzer-Stenner, R. (2006) The conformations adopted by the octamer peptide $(AAKA)_2$ in aqueous solution probed by FTIR and polarized Raman spectroscopy, *J. Raman Spectrosc. 37*, 248−254.
70. Pappu, R. V., and Rose, G. D. (2002) A simple model for polyproline II structure in unfolded states of alanine-based peptides, *Protein Sci. 11*, 2437−2455.
71. Asher, S. A., Mikhonin, A. V., and Bykov, S. (2004) UV Raman demonstrates that α-helical polyalanine peptides melt to polyproline II conformations, *J. Am. Chem. Soc. 126*, 8433−8440.
72. Swindells, M. B., MacArthur, M. W., and Thornton, J. M. (1995) Intrinsic ϕ,ψ propensities of amino acids, derived from the coil regions of known structures, *Nat. Struct. Biol. 2*, 596−603.
73. Graf, J., Nguyen, P. H., Stock, G., and Schwalbe, H. (2007) Structure and dynamics of the homologous series of alanine peptides: a joint molecular-dynamics/NMR study, *J. Am. Chem. Soc.* (in press).

BI062224L